doi:10.1093/brain/awaa102 BRAIN 2020: 143; 1431–1446 | 1431

BRAIN
A JOURNAL OF NEUROLOGY

Myelin oligodendrocyte glycoprotein antibody-associated disease: an immunopathological study

Yoshiki Takai,[1] Tatsuro Misu,[1,2] Kimihiko Kaneko,[1,3] Norio Chihara,[4] Koichi Narikawa,[5] Satoko Tsuchida,[6] Hiroya Nishida,[7] Takashi Komori,[8] Morinobu Seki,[9] Teppei Komatsu,[10] Kiyotaka Nakamagoe,[11] Toshimasa Ikeda,[12] Mari Yoshida,[12] Toshiyuki Takahashi,[13] Hirohiko Ono,[1] Shuhei Nishiyama,[1] Hiroshi Kuroda,[1] Ichiro Nakashima,[14] Hiroyoshi Suzuki,[15] Monika Bradl,[16] Hans Lassmann,[16] Kazuo Fujihara[1,17] and Masashi Aoki[1] on behalf of the Japan MOG-antibody Disease Consortium*

*Appendix 1.

Conformation-sensitive antibodies against myelin oligodendrocyte glycoprotein (MOG) are detectable in patients with optic neuritis, myelitis, opticomyelitis, acute or multiphasic disseminated encephalomyelitis (ADEM/MDEM) and brainstem/cerebral cortical encephalitis, but are rarely detected in patients with prototypic multiple sclerosis. So far, there has been no systematic study on the pathological relationship between demyelinating lesions and cellular/humoral immunity in MOG antibody-associated disease. Furthermore, it is unclear whether the pathomechanisms of MOG antibody-mediated demyelination are similar to the demyelination patterns of multiple sclerosis, neuromyelitis optica spectrum disorders (NMOSD) with AQP4 antibody, or ADEM. In this study, we immunohistochemically analysed biopsied brain tissues from 11 patients with MOG antibody-associated disease and other inflammatory demyelinating diseases. Patient median onset age was 29 years (range 9–64), and the median interval from attack to biopsy was 1 month (range 0.5–96). The clinical diagnoses were ADEM ($n = 2$), MDEM ($n = 1$), multiple brain lesions without encephalopathy ($n = 3$), leukoencephalopathy ($n = 3$) and cortical encephalitis ($n = 2$). All these cases had multiple/extensive lesions on MRI and were oligoclonal IgG band-negative. Most demyelinating lesions in 10 of 11 cases showed a perivenous demyelinating pattern previously reported in ADEM (153/167 lesions) and a fusion pattern (11/167 lesions) mainly in the corticomedullary junctions and white matter, and only three lesions in two cases showed confluent demyelinated plaques. In addition, 60 of 167 demyelinating lesions (mainly in the early phase) showed MOG-dominant myelin loss, but relatively preserved oligodendrocytes, which were distinct from those of AQP4 antibody-positive NMOSD exhibiting myelin-associated glycoprotein-dominant oligodendrogliopathy. In MOG antibody-associated diseases, MOG-laden macrophages were found in the perivascular spaces and demyelinating lesions, and infiltrated cells were abundant surrounding multiple blood vessels in and around the demyelinating lesions, mainly consisting of macrophages (CD68; 1814 ± 1188 cells/mm^2), B cells (CD20; 468 ± 817 cells/mm^2), and T cells (CD3; 2286 ± 1951 cells/mm^2), with CD4-dominance (CD4+ versus CD8+; 1281 ± 1196 cells/mm^2 versus 851 ± 762 cells/mm^2, $P < 0.01$). Humoral immunity, evidenced by perivascular deposits of activated complements and immunoglobulins, was occasionally observed in some MOG antibody-associated demyelinating lesions, and the frequency was much lower than that in AQP4 antibody-positive NMOSD. Subpial lesions with perivenous demyelination were observed in both ADEM and cortical encephalitis. Our study suggests that ADEM-like perivenous inflammatory demyelination with MOG-dominant myelin loss is a characteristic finding of MOG antibody-associated disease regardless of whether the diagnostic criteria of ADEM are met. These pathological features are clearly different from those of multiple sclerosis and AQP4 antibody-positive NMOSD, suggesting an independent autoimmune demyelinating disease entity.

Received February 22, 2019. Revised July 31, 2019. Accepted February 17, 2020

1 Department of Neurology, Tohoku University Graduate School of Medicine, Sendai, Miyagi, Japan
2 Department of Multiple Sclerosis Therapeutics, Tohoku University Graduate School of Medicine, Sendai, Miyagi, Japan
3 Department of Neurology, National Hospital Organization Miyagi National Hospital, Watari, Miyagi, Japan
4 Division of Neurology, Kobe University Graduate School of Medicine, Kobe, Hyogo, Japan
5 Department of Neurology, Japanese Red Cross Ishinomaki Hospital, Ishinomaki, Miyagi, Japan
6 Department of Pediatrics, Japanese Red Cross Akita Hospital, Akita, Akita, Japan
7 Department of Neuropediatrics, Tokyo Metropolitan Neurological Hospital, Fuchu, Tokyo, Japan
8 Department of Laboratory Medicine and Pathology, Tokyo Metropolitan Neurological Hospital, Fuchu, Tokyo, Japan
9 Department of Neurology, Keio University School of Medicine, Shinjuku-ku, Tokyo, Japan
10 Department of Neurology, the Jikei University School of Medicine, Minato-ku, Tokyo, Japan
11 Department of Neurology, Division of Clinical Medicine, Faculty of Medicine, University of Tsukuba, Tsukuba, Ibaraki, Japan
12 Department of Neuropathology, Institute for Medical Science of Aging, Aichi Medical University, Nagakute, Aichi, Japan
13 Department of Neurology, National Hospital Organization Yonezawa National Hospital, Yonezawa, Yamagata, Japan
14 Department of Neurology, Tohoku Medical and Pharmaceutical University, Sendai, Miyagi, Japan
15 Department of Pathology, National Hospital Organization Sendai Medical Center, Sendai, Miyagi, Japan
16 Department of Neuroimmunology, Center for Brain Research, Medical University of Vienna, Vienna, Austria
17 Department of Multiple Sclerosis Therapeutics, Fukushima Medical University, Fukushima, Fukushima, Japan

Correspondence to: Dr Tatsuro Misu
Department of Neurology, Tohoku University Graduate School of Medicine, Sendai 980-8574,
Japan
E-mail: misu@med.tohoku.ac.jp

Keywords: myelin oligodendrocyte glycoprotein; acute disseminated encephalomyelitis; antibody; perivenous demyelination; pattern-II multiple sclerosis

Abbreviations: ADEM = acute disseminated encephalomyelitis; MDEM = multiphasic disseminated encephalomyelitis; NMOSD = neuromyelitis optica spectrum disorder; TDD = tumefactive demyelinating disease

Introduction

Myelin oligodendrocyte glycoprotein (MOG) is a myelin protein exclusively expressed at the outermost surface of the myelin sheath and oligodendrocyte membranes in the CNS (Johns and Bernard, 1999). MOG is a member of the immunoglobulin superfamily and one of the best-studied autoantigens involved in experimental autoimmune encephalomyelitis (EAE), and MOG-EAE is an animal model of inflammatory demyelinating disease with the primary and secondary production of MOG-specific lymphocytes and MOG antibodies (Reindl *et al.*, 2013; Ramanathan *et al.*, 2016; Peschl *et al.*, 2017*a*). Thus, MOG antibody had long been considered a potentially pathogenic autoantibody involved in human inflammatory demyelinating diseases, especially multiple sclerosis, but previous results on the detection of MOG antibody by ELISA or western blot were confusing because of the low specificity. However, by using cell-based assays, it has become clear that the conformation-sensitive MOG antibody is detectable in a proportion of patients with such inflammatory CNS demyelinating diseases as optic neuritis, acute myelitis, neuromyelitis optica spectrum disorder (NMOSD) without aquaporin-4 (AQP4) antibody (Kitley *et al.*, 2012; Sato *et al.*, 2014), acute disseminated encephalomyelitis (ADEM) (Di Pauli *et al.*, 2011), multiphasic DEM (MDEM) and cerebral cortical encephalitis (Fujimori *et al.*, 2017; Ogawa *et al.*, 2017). Meanwhile, patients with typical multiple sclerosis are essentially negative for the MOG antibody (Ketelslegers *et al.*, 2015; Waters *et al.*, 2015). Some previous case reports on biopsied brain lesions in patients with MOG antibodies highlighted the deposition of complement components and concluded that the lesions were characterized by humoral immune-mediated demyelination of multiple sclerosis (multiple sclerosis pathology pattern II) (Lucchinetti *et al.*, 2000; Spadaro *et al.*, 2015; Jarius *et al.*, *2016a*, *b*; Kortvelyessy *et al.*, 2017). However, pathological studies on the relationships between cellular and humoral immunity and demyelinating lesions were insufficient in MOG antibody-associated disease. It is also unclear whether demyelinating plaques in cases with MOG antibodies show confluent demyelination; confluent demyelination is seen in multiple sclerosis, but it is rarely observed in classic ADEM cases (Young *et al.*, 2010). As some previous studies on EAE have demonstrated that the ratios of myelin antigen-specific lymphocytes and autoantibodies to myelin could influence the dominance of perivenous or confluent demyelination (Lassmann *et al.*, 1988; Linington *et al.*, 1988), it would be interesting to analyse whether the balance of cellular and humoral immunities and the pattern of inflammatory demyelination are relevant in human diseases. In addition, there have been few pathological analyses that have sought to determine whether MOG is specifically targeted and damaged in MOG antibody-associated disease.

In this study, we aimed to analyse the pathology of MOG antibody-associated diseases from the following three angles: (i) determining whether the pattern of MOG antibody-associated demyelinating lesions shows multiple sclerosis-like

confluent demyelination or ADEM-like perivenous demyelination; (ii) determining the relationship between humoral/cellular immune components and demyelinating plaques in MOG antibody-associated disease; and (iii) determining the presence or absence of preferential damage to MOG in MOG antibody-associated demyelination.

Materials and methods

Patients

We analysed 11 brain biopsies from patients with MOG antibody-positive diseases, which are summarized in Table 1. All patients were examined for MOG antibody and AQP4 antibody status by our in-house cell-based assays, as reported previously (Takahashi *et al.*, 2006; Kaneko *et al.*, 2018). The brain biopsies were performed between December 2004 and July 2018 at Tohoku University Hospital ($n = 2$), Japanese Red Cross Ishinomaki Hospital ($n = 1$), Japanese Red Cross Akita Hospital ($n = 1$), Tokyo Metropolitan Neurological Hospital ($n = 1$), Kobe University Hospital ($n = 2$), Keio University Hospital ($n = 1$), Tsukuba University Hospital ($n = 1$), Jikei University Hospital ($n = 1$), and Aichi Medical University Hospital ($n = 1$). For a comparative study, we also analysed brain biopsies from patients with ADEM ($n = 5$) and tumefactive demyelinating disease (TDD) with confluent demyelination ($n = 4$) and from autopsied patients with classic multiple sclerosis ($n = 11$) and AQP4 antibody-positive NMOSD ($n = 8$). As a neurological disease control, patients with non-inflammatory disorders (amyotrophic lateral sclerosis, Huntington's disease, cardiac infarction; $n = 1$, each) and cerebral infarction ($n = 3$) were also analysed.

MOG- and AQP4-antibody assays

Each patients' serum was analysed using a cell-based assay with live human embryonic kidney 293 (HEK-293) cells stably transfected with the M23 isoform of AQP4 for the AQP4 antibody assay, and stably transfected with full-length human *MOG* cDNA (pIRES2-Dsred2 vector, BD Biosciences; provided by P.J.W.) for MOG antibody assay. Goat anti-human IgG Fc labelled with DyLight™ 488 (Thermo Scientific) was used as a secondary antibody after the transfected cells were exposed to the patients' diluted sera. The titres of MOG antibody were calculated semi-quantitatively using consecutive 2-fold dilutions, and patients were only judged to be positive when the fluorescent colour of DyLight™ 488 was confirmed at a minimum dilution of 1:128.

Neuropathological examinations and immunohistochemistry

In the neuropathological examinations, 4–5-μm thick slices of paraffin-embedded biopsied or autopsied tissues were evaluated by standard neuropathological methods, including haematoxylin and eosin and Klüver–Barrera staining and by immunohistochemical techniques, including EnVision (Dako) or Histofine® Simple Stain™ kit (Nichirei), with specific markers for myelin sheaths, oligodendrocytes, axons, astrocytes, complement components, immunoglobulins and inflammatory cells (T and B cells, macrophages). The primary antibodies and specific conditions used for immunohistochemistry in this study are summarized in Supplementary Table 1.

Briefly, the paraffin-embedded sections were deparaffinized in xylene and rehydrated in ethanol. After rinsing with phosphate-buffered saline (PBS), antigen retrieval was performed by heating the sections at an adequate temperature for the prescribed length of time in the heat retrieval solution Diva Decloaker (Biocare Medical) in a decloaking chamber (model DC2002, Biocare Medical). After blocking non-specific binding with 10% goat serum for 15 min at room temperature, the slides were covered and incubated with primary antibodies at 4°C overnight. The slides were washed with PBS and incubated with 30% methanol/PBS containing 1% H_2O_2 for 20 min to block endogenous peroxidase, after which they were washed three times with PBS. Secondary antibodies were applied and incubated for 40 min at room temperature.

For staining, we used diaminobenzidine hydrochloride (DAB) (brown) for the horseradish peroxidase system, and fuchsin (Dako) (red) or Vector blue (Vector) (blue) for the alkaline phosphatase (AP) system. Selected sections were counterstained with haematoxylin (blue) or nuclear fast red (Vector) (red). For double staining, we combined two enzyme systems, horseradish peroxidase and alkaline phosphatase.

Lesion evaluation

All glass slides with tissue slices were converted into high-resolution digital data with a special scanner (NanoZoomer-SQ) and evaluated on the dedicated viewing software (NDP.view2, Hamamatsu, Japan). We classified every demyelinating lesion into either the confluent pattern (multiple sclerosis-like) or perivenous pattern (ADEM-like) based on the Klüver–Barrera staining or immunohistochemical analysis of myelin basic protein (MBP), myelin associated glycoprotein (MAG) or MOG, and then we counted the number of vessels present in these demyelinating plaques. Demyelinating lesions with stained areas of 1000 μm^2 or larger were evaluated. The pathology of perivenous demyelination was defined as myelin loss with indistinct margins that surrounded a small vessel associated with inflammatory infiltrates (Young *et al.*, 2010; Koelman and Mateen, 2015), and confluent demyelination was pathologically defined as a demyelinating plaque with an extensive, well-demarcated leading edge and with preserved axons and reactive astrocytes, containing a number of vessels. We also evaluated the relationships between each demyelinating lesion and humoral immune factors or inflammatory cell infiltration in adjacent tissue slices (within a radius of 50 μm). For the cell count of perivascular cuffing, 4–10 blood vessels with inflammatory cell infiltration were randomly extracted for each case, and the average value of the cell number per square millimetre was calculated.

Statistical analysis

Paired *t*-tests were used to compare the numbers of CD4+ and CD8+ T cells. Tukey's multiple comparison test was used to compare the phagocytic activity of macrophages in each disease. All statistical analyses were conducted with GraphPad Prism 5 (GraphPad Software Inc., San Diego, CA), and $P < 0.05$ was considered statistically significant.

Table 1 Clinical, MRI and laboratory data in 11 brain-biopsied patients with MOG antibody-associated disease

Pt	Phenotype	Age/ sex	Attacks (at biopsy/ total)	Symptoms	MRI lesions								Biopsy site	Time from attack to biopsy (m)	Total FU period (m)	MOG titre[a]	CSF OB	Treatment	
					Co	WM	BG	DE	Ce	BS	SC	ON						Before biopsy	After biopsy
1	ADEM	24/M	1st/2	Seizure, DOC, dysarthria, aphasia	+	++	+	–	–	+	–	–	L temporal	2	42	512	–	AED	IVMP, OP
2	Multiple brain lesion	9/M	1st/1	L visual impairment, L hemiparesis	±	+++	++	+	–	+	–	+	L parieto-temporal	1	19	2048	–	None	IVMP, OP
3	Leukoencephalopathy	16/F	progressive	seizure, cognitive behavioural dysfunction, tetraparesis	–	+++	–	+	–	±	–	–	R frontal	96	132	2048	–	AED	IVMP, OP, IVIg
4	Multiple brain lesion	33/M	1st/1	Fever, seizure, upper gaze restriction, paraparesis	±	++	–	+	–	–	–	–	Bi parietal	1	36	1024	–	AED	IVMP, OP
5	ADEM	64/F	1st/1	DOC, headache, visual impairment, apraxia, ataxia, tetraparesis	+	+	–	+	–	++	–	+	L parietal	0.5	23	16384	–	None	IVMP, OP
6	Cortical encephalitis	15/F	1st/1	Headache, nausea, seizure, amnesic aphasia	++	+	–	–	–	–	–	–	L temporal	0.75	14	512	–	IVMP, AED	IVMP, OP
7	Leukoencephalopathy	47/M	1st/1	Fever, headache, DOC, L ocular palsy, L facial palsy, hypaesthesia in Bi L/Es	–	+++	–	±	+	+	+	±	R occipital	2	19	4096	–	None	IVMP, PE, OP
8	MDEM	28/F	2nd/3	Seizure, abnormal behaviour, R hemiparesis	±	++	++	–	–	+	–	–	L frontal	1	180	128	–	OP	IVMP, OP
9	Leukoencephalopathy	44/F	1st/1	Status epilepticus, semicoma, tetraparesis	+	+++	+	±	±	++	+	–	R frontal	5	12	1024	–	IVMP, OP, PE, IVIg, CyA	IVMP, OP, IVCY
10	Multiple brain lesion	62/M	4th/5	Dizziness, L visual impairment, L hemiparesis	–	++	±	–	–	–	–	+	R corpus callosum	0.75	56	256	–	None	IVMP, OP
11	Cortical encephalitis	29/F	1st/1	Fever, seizure, visual loss	+	–	–	–	–	–	–	+	R parietal gyrus	0.75	33	1024	–	None	IVMP, OP

MRI lesions: - = no lesion; ± = equivocal lesion; + = one small or moderate-sized lesion; ++ = multiple moderate-sized lesions or one tumefactive lesion (>2 cm); +++ = multiple tumefactive lesions (>2 cm).
AED = anti-epilepsy drug; BG = basal ganglia; Bi = bilateral; BS = brainstem; Ce = cerebellum; Co = cortical; CyA = cyclosporine; DE = diencephalon; DOC = disturbance of consciousness; F = female; FU = follow-up; IVCY = intravenous cyclophosphamide; IVIg = intravenous immunoglobulin; IVMP = intravenous methylprednisolone; L = left; L/E = lower extremity; M = male; m = month(s); OB = oligoclonal IgG bands; ON = optic nerve; OP = oral prednisolone; PE = plasmapheresis; Pt = patient; R = right; SC = spinal cord; WM = white matter.
[a]MOG antibody was measured at the following times in each case (after onset): Patient 1, 2 months; Patient 2, 1 month; Patient 3, 96 months; Patient 4, 2 months; Patient 5, 1 month; Patient 6, 1 month; Patient 7, 3 months; Patient 8, 1 month; Patient 9, 1 month; Patient 10, 32 months; Patient 11, 4 months.

Standard protocol approvals, registration, and patient consent

This multi-institutional study was approved by the ethics committees of Tohoku University and the institutes with which the other co-investigators are affiliated and was conducted in accordance with the internationally recognized ethical standards. All study participants provided written informed consent.

Data availability

The datasets that support the findings of the current study are available from the corresponding author on reasonable request. The data are not publicly available because they contain information that could compromise the privacy of research participants.

Results

MOG antibody-associated disease

Clinical presentation and MRI findings

The patients' median age at onset was 29 years (range 9–64), and five patients were male. The clinical diagnoses were ADEM in two patients, MDEM in one, multiple brain lesions without encephalopathy in three, leukoencephalopathy in three and cortical encephalitis in two. Brain biopsies were performed at their first attack in eight patients, and the majority of brain biopsies were performed before the initiation of acute phase treatment. The median interval from onset or relapse to biopsy was 1 month (range 0.5–96). All patients were positive for MOG antibody (range 128×–16 384×) at least once. MOG antibody was persistently positive in five cases, while two cases converted to negative during the follow-up periods. Oligoclonal IgG bands were negative in all MOG antibody-positive cases. Only Patient 3, who had progressive leukoencephalopathy, had a co-existing antibody (anti-*N*-methyl-D-aspartate receptor antibody). Brain MRI was performed before biopsy in all patients, and the findings are shown in Fig. 1. Partial clinical and pathological data for Patients 7 and 11 were reported previously (Ikeda *et al.*, 2018; Komatsu *et al.*, 2019). Brain MRI abnormalities in our MOG antibody-positive patients were multifocal diffuse or spotty T_2 hyperintense lesions with multiple patchy or linear gadolinium enhancement, and these brain lesions were disseminated in space, although most lesions developed concurrently, which is different from lesions in prototypic multiple sclerosis, which are typically accompanied by an open ring-like contrast enhancement.

General pathology

We obtained brain biopsy specimens with sizes ~1.5 mm × 5 mm when obtained by stereotactic needle biopsy or ~8–10 mm^2 when obtained by open biopsy. In the haematoxylin and eosin staining, these tissues showed relatively severe inflammation with tissue oedema and reactive astrogliosis in the absence of marked haemorrhage, ischaemic necrosis, or malignancy. With Klüver–Barrera staining, most lesions were seen as perivenous sleeves of demyelination with indistinct borders but with preservation of axon. In cases with multiple demyelinating lesions, the lesions tended to be in the same lesion stages and were occasionally accompanied with massive perivenous infiltrations of mononuclear cells and/or macrophages, but less polymorphonuclear cells. In a few cases, there were coalescing perivenous demyelinating lesions consisted of a few to several perivenous lesions. The staining of neurofilament was preserved in the lesions.

In the present 11 patients, the demyelinated lesions were located at the cortico-medullary junctions and leptomeningeal areas of the cortex as well as the cerebral white matter. In most perivenous demyelinating lesions, many macrophages were infiltrated and phagocytic macrophages were occasionally observed. Meanwhile, in a few confluent demyelinating lesions (Patient 7), we observed many phagocytic macrophages at the periphery of the demyelinating plaques. Astroglial activation was noticeable and extensive in and around the demyelinated lesions. We occasionally found markedly enlarged hypertrophic astrocytes with no abnormal mitosis, but Creutzfeldt-Peters cells were not observed. There were cortical microglial activation and aggregation in some areas of the grey matter.

Demyelination pattern in the cerebral white matter

We evaluated 167 demyelinating lesions with blood vessels in the cerebral white matter and 209 vessels in the lesions. Among them, a majority of demyelinating lesions in 10 of 11 cases showed the perivenous demyelinating pattern (153/167 lesions) (Table 2), as previously reported in patients with ADEM (Fig. 2A and B). Only two lesions in one patient (Patient 7, each plaque contained four and six vessels) showed confluent demyelination with active leading edges, but he had 24 perivenous demyelinating lesions. In Patient 9, all areas in the specimens were demyelinated; therefore, we judged that this lesion displayed confluent demyelination. The remaining lesions were large, but not uniformly demyelinating, appearing to result from the fusion of perivascular demyelinating lesions (11/167 lesions) in six cases (Table 2). Among them, 60 of 167 demyelinating lesions (mostly in the early phase) showed MOG-dominant myelin loss rather than other types of myelin protein losses (Figs 2C–E, 3 and Supplementary Fig. 1A–D), and some of these MOG-dominant demyelinating lesions also displayed IgG deposition.

All vessels in the demyelinating lesions were accompanied by macrophages (1814 ± 1188 cells/mm^2), and myelin phagocytic macrophages were seen not only in the demyelinating plaques, but also in the perivascular space (50/209 vessels). Interestingly, MOG-dominant debris and some macrophages phagocytosing the debris were observed in the perivascular space in 13 of 346 vessels localized in and around the demyelinating plaques in eight patients (Fig. 2F–H). Perivascular cuffs in and around the demyelinating lesions contained many T cells (CD3; 2286 ± 1951 cells/mm^2), while B cell infiltration was less pronounced (CD20; 468 ± 817 cells/mm^2). Infiltrating T cells were

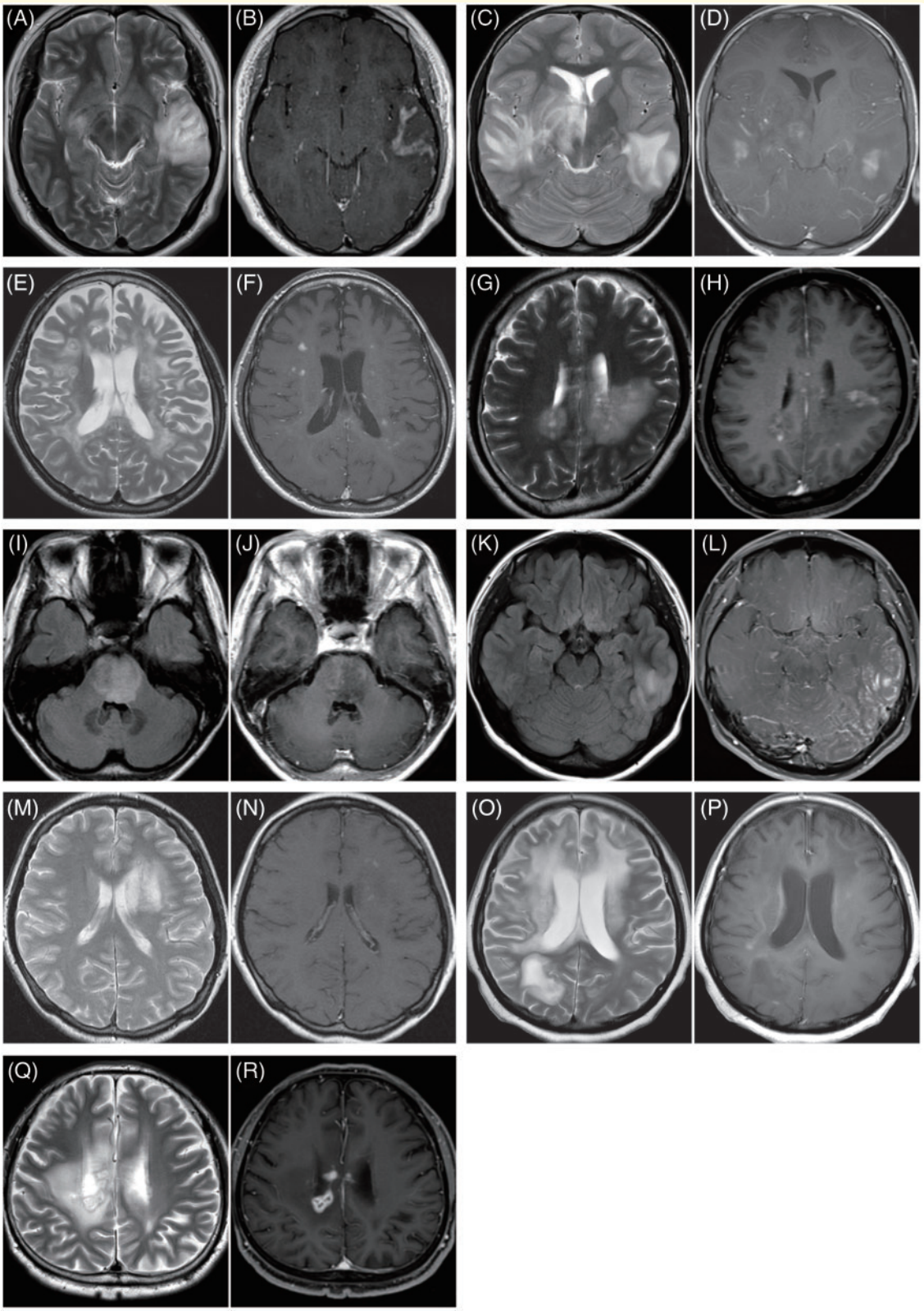

Figure 1 Brain MRI of the patients with MOG antibody-associated disease. (**A** and **B**) Patient 1, ADEM. T_2-weighted imaging (T2WI) revealed a large hyperintense lesion extending from the cortex to the subcortical white matter in the left temporal lobe (**A**). The lesion was Gd-enhanced in the subcortical white matter, but it partially extended into the cortex (**B**) [T2WI (**A**); Gd-T1WI (**B**)]. (**C** and **D**) Patient 2, multiple brain lesions. Large T_2-hyperintense lesions were visible in the bilateral temporal lobes with the right-sided lesion extending to the right basal ganglia and thalamus (**C**). Contrast enhancements were mainly located in the white matter (**D**) [T2WI (**C**); Gd-T1WI (**D**)]. (**E** and **F**) Patient 3, leukoencephalopathy. Extensive T_2 hyperintense lesions (**E**) were localized in the deep cerebral white matter with multiple punctate

(continued)

dominated by CD4+ cells (CD4+ versus CD8+; 1281 ± 1196 cells/mm^2 versus 851 ± 762 cells/mm^2, $P < 0.01$), (Fig. 2I–L). Meanwhile, perivascular depositions of activated complement components were observed only in a vessel in the demyelinating lesion without vasculocentric pattern (Patient 5), and there were only four demyelinating lesions associated with debris-like activated complement components in macrophages (Patient 7). In addition, immunoglobulin G staining was observed in the perivenous areas of demyelinating lesions in seven cases (Fig. 5).

Demyelination pattern in the cortico-medullary junctions

We evaluated the subpial tissues and cortico-medullary junctions in seven patients. Among them, three (Patients 1, 6 and 11) showed demyelinating lesions with preferential loss of MOG, in the cortico-subcortical tissues (Fig. 4A–D). The oligodendrocytes and axons were well preserved in these lesions (Fig. 4E and F) but were accompanied by activated astrocytes (Fig. 4G), macrophages and activated microglia (Fig. 4H), T cells and fewer B cells (Fig. 4I and J). Cortical microglial activation and aggregation were seen in some areas of the grey matter (Supplementary Fig. 2A and B). Several perivenous demyelinating lesions were observed at the corticomedullary junction and at the border of subpial demyelination (Supplementary Fig. 2C–G). We found only small amounts of IgG and minor debris-like deposition of activated complement components in the lesions (Fig. 4K and L), but some perivenous focal lesions with MOG-dominant myelin loss located at the cortico-medullary junctions showed IgG deposition without activated complement components (Fig. 5). Myelin loss was also seen in the subpial area (Fig. 4M and N as control) with reactive astrocytes localized subpially (Fig. 4O). The demyelinating areas were accompanied by T cell-dominant inflammatory cell infiltration at the meninges (Fig. 4P and Q). The pathological findings for individual MOG antibody-positive patients are summarized in Table 2.

Relationship between clinical manifestations and patterns of demyelination

In this study, there were six patients who showed ADEM-like multiple white matter lesions with or without cortical involvement in their MRI findings (Patients 1, 2, 4, 5, 8 and 10). The pathological findings of these patients were mainly perivenous demyelination. Two of three patients diagnosed as leukoencephalopathy whose MRI showed large and diffuse white matter lesions (Patients 7 and 9), had large demyelinating lesions in their brain biopsy specimens.

Patient 9 was atypical and an intractable case in which extensive white matter lesions progressed on serial brain MRI during several months from the onset, despite various immunological treatments. These findings were different from those of prototypic multiple sclerosis. In the pathological analysis, brain biopsy was performed at an advanced stage, and the tissue was mostly demyelinated. For that reason, we tentatively classified this patient's lesions into a confluent pattern, but we could not analyse the demyelinating patterns in detail.

Patient 7 was the only case with multiple sclerosis-like confluent demyelinating lesions, which might have resulted from several fused perivenous lesions. However, he had no relapse during a 2-year follow-up period and there were no periventricular ovoid lesions or oligoclonal IgG bands in the CSF. In addition, the patient also had a number of perivenous demyelinating lesions (Table 2), which is consistent with pathology of ADEM.

Interestingly, in addition to the two cases of cortical encephalitis (Patients 6 and 11), one patient diagnosed with ADEM (Patient 1) exhibited a similar pattern of subpial demyelination, suggesting they may belong to the same pathological entity despite different clinical and MRI phenotypes.

Moreover, there were three cases with two or more attacks (Table 1) in whom multiple sclerosis might be suspected. Patient 1 who had diffuse ADEM-like lesions had a second clinical attack manifesting trigeminal neuralgia, but no brainstem lesion corresponding to the symptom was detected by brain MRI. Patient 8 had three episodes including two with disseminated brain lesions and one with large brainstem lesions, but she never developed multiple sclerosis-like ovoid lesions during 15-year follow-up. Patient 10 developed dysarthria and vertigo at onset and then had four more clinical episodes. In these episodes, diffuse white matter lesions developed but they resolved completely following corticosteroid therapy. Meanwhile, no multiple sclerosis-like ovoid lesions were seen during

Figure 1 Continued

Gd-enhanced lesions (**F**) [T2WI (**E**); Gd-T1WI (**F**)]. (**G** and **H**) Patient 4, multiple brain lesions. Two large pale T_2-hyperintense lesions were visible with patchy, slightly brighter T_2-hyperintensities around the lateral ventricles (**G**). Gd enhancement was observed at the periphery (**H**) [T2WI (**G**); Gd-T1WI (**H**)]. (**I** and **J**) Patient 5, ADEM. A large pontine FLAIR-hyperintense lesion was seen (**I**) with pale contrast enhancement in the periphery (**J**) [FLAIR (**I**); Gd-T1WI (**J**)]. (**K** and **L**) Patient 6, cortical encephalitis. Left temporal cortex and adjacent subcortical area showed FLAIR-hyperintensity (**K**). Gd-enhancement was observed in the meninges along the cerebral sulci (**L**) [FLAIR (**K**); Gd-T1WI (**L**)]. (**M** and **N**) Patient 8, MDEM. A large T_2 hyperintense lesion was located in the left frontal white matter adjacent to the anterior horn of the lateral ventricle (**M**). Multiple faint Gd-enhancements were observed inside the lesion (**N**) [T2WI (**M**); Gd-T1WI (**N**)]. (**O** and **P**) Patient 9, leukoencephalopathy. Multiple extensive T_2 hyperintense lesions (**O**) with marginal Gd-enhancement (**P**) were seen in the bilateral deep cerebral white matter [T2WI (**O**); Gd-T1WI (**P**)]. (**Q** and **R**) Patient 10, cortical encephalitis. Large T_2-hyperintense lesions (**Q**) with several small ring-shaped Gd-enhancements (**R**) were visible around the right lateral ventricle [T2WI (**Q**); Gd-T1WI (**R**)]. FLAIR = fluid-attenuated inversion recovery images; Gd-T1WI = post-Gd T_1-weighted images; T2WI = T_2-weighted images.

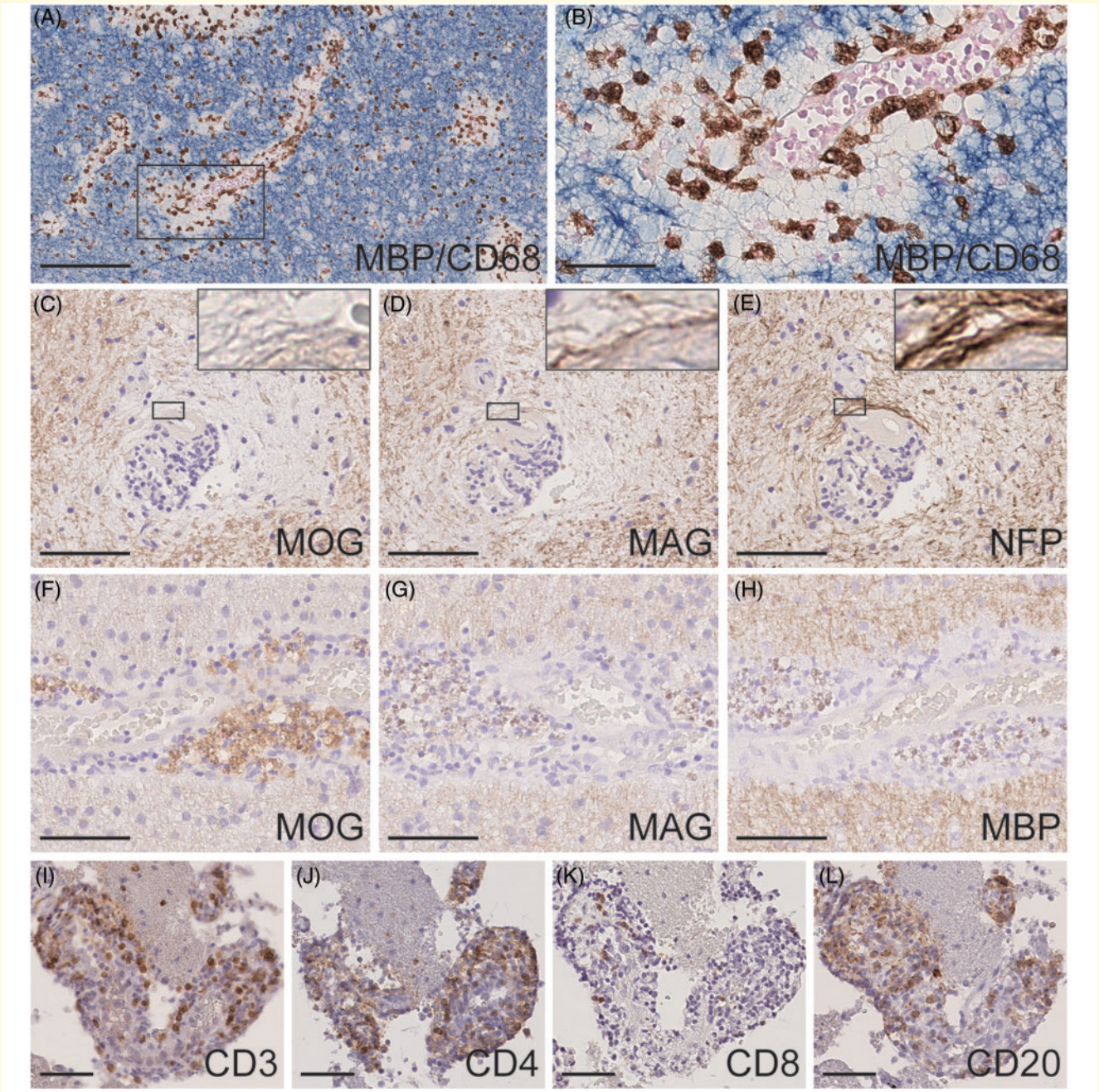

Figure 2 Characteristic features of demyelination in the white matter in MOG antibody-associated disease. (**A** and **B**) Multiple ADEM-like perivenous demyelination [loss of MBP staining (blue)] accompanied by a number of CD68+ macrophages (brown) (Patient 5). Scale bar = 200 μm. (**B**) High magnification image of the boxed area in **A**, showing perivenous activity of phagocytic macrophages. Scale bar = 50 μm. (**C**–**E**) MOG-dominant perivenous demyelination. The loss of MOG staining (**C**) was more extensive than the loss of MAG staining (**D**), while the staining of NFP+ axons (**E**) was relatively preserved compared with the extent of demyelination. Patient 7, scale bar = 80 μm. *Inset*: Higher magnification images of MOG-dominant perivenous demyelination adjacent to a blood vessel indicated by a rectangle in each figure. (**F**–**H**) In surrounding areas of demyelinating lesions, MOG-dominant debris and MOG-laden macrophages were observed dominantly in the perivascular space (**F**), while such findings were much less evident in MAG (**G**) and MBP (**H**) (Patient 1). Scale bar = 80 μm. (**I**–**L**) Perivascular cuffing was mainly composed of T cells dominated by CD4+ (**J**) rather than CD8+ cells (**K**). CD20+ B cells were also found (Patient 2). Scale bar = 50 μm. NFP = neurofilament protein.

5-year period. Pathologically, these cases had some fused demyelinating lesions (Table 2), but they have never been diagnosed with multiple sclerosis.

These cases had some ADEM-like perivenous lesions with fused or confluent demyelinated lesions but were without typical features of multiple sclerosis, suggesting that they

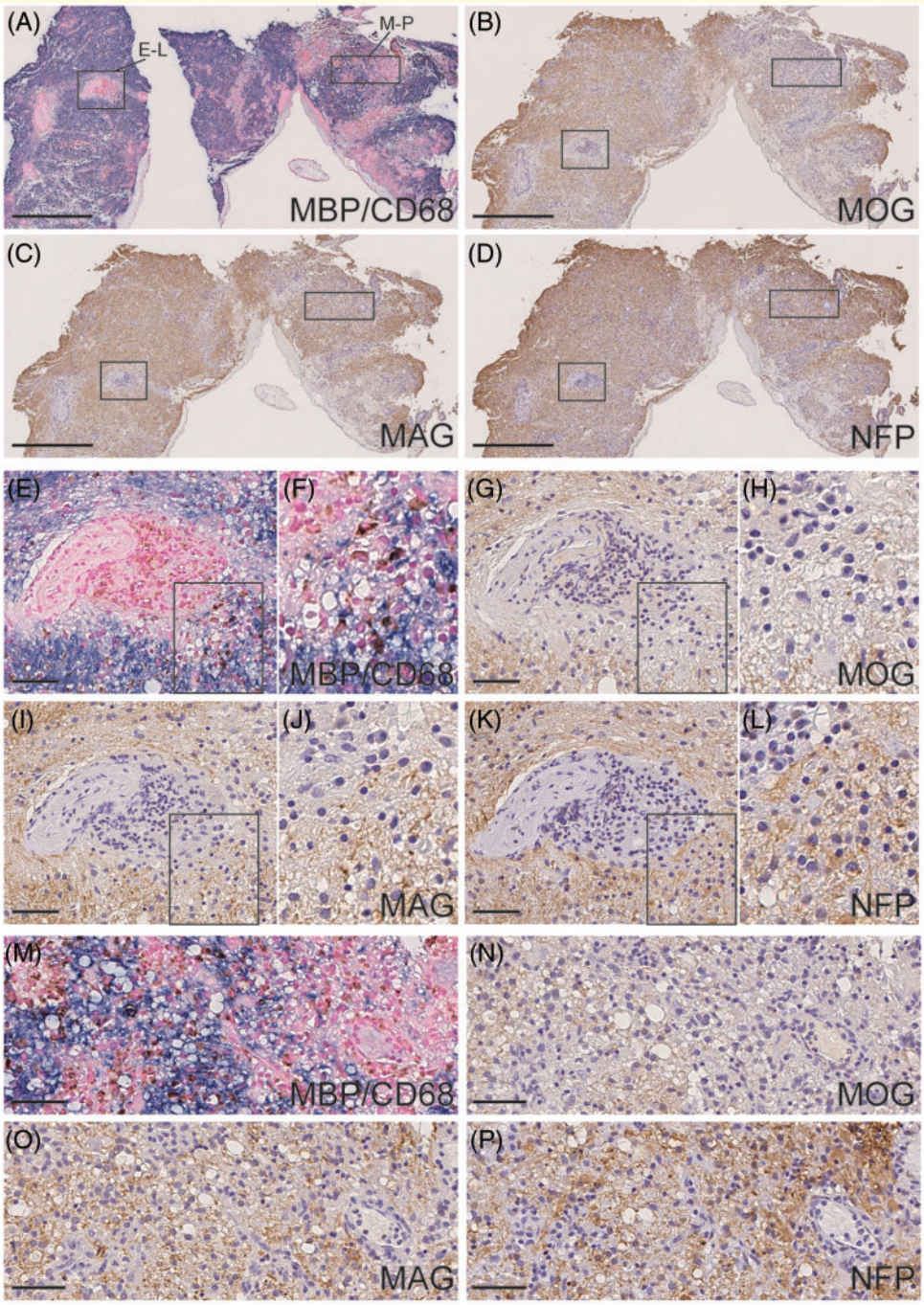

Figure 3 The isolated and fusion pattern of perivenous demyelination with MOG-dominant myelin loss in acute MOG antibody-associated disease. (**A**–**D**) The isolated perivenous demyelination (**E**–**L**) and fusion pattern of perivenous demyelination (**M**–**P**). There was multiple/disseminated perivenous demyelination where loss of MOG staining (**B**) was more extensive than loss of MBP (**A**, blue) and MAG (**C**) staining, while the staining of NFP+ axons (**D**) was relatively preserved (Patient 8). Scale bar = 500 μm. (**E**, **G**, **I** and **K**) High magnification images of a selected areas from **A**–**D**, with even higher magnification images of a selected area indicated by a rectangle in **E**, **G**, **I** and **K** (**F**, **H**, **J** and **L,** respectively). A number of inflammatory cells and CD68+ macrophages were infiltrated around a vessel (**E** and **F**) and were accompanied with perivenous MOG-dominant myelin loss and a few myelin-laden macrophages (**G** and H). Meanwhile, MBP (**E** and **F**) and MAG (**I** and **J**), and axons (**K** and **L**) were relatively preserved. Scale bar = 50 μm. (**M** and **P**) High magnification images of a selected area were shown as **M** and **P** in **A**–**D**. Double staining of myelin (MBP, blue) and macrophages (CD68, brown) showed fused pattern of multiple perivenous demyelination with massive infiltration of myelin-phagocytic macrophages indicating active demyelination (**M**). MOG staining showed relatively large coalescent demyelinating lesions with some MOG-laden macrophages suggesting MOG-dominant demyelination (**N**), compared to MBP (**M**) and MAG stainings (**O**). Some axons (**P**) located in these lesions showed axonal swelling but well preserved compared to myelin sheaths. Scale bar = 500 μm. NFP = neurofilament protein.

Table 2 Neuropathological findings in 11 brain-biopsied patients with MOG antibody-associated disease

Patient	Demyelination pattern	MOG dominant loss		Immune cells infiltrating in perivascular cuffings				
		White matter	Subpial	T cell			B cell	Macrophage
				CD3	CD4	CD8	CD20	CD68
1	2 perivenous 1 subpial	0/2	1/1	54.2 (14.3)	28.7 (8.6)	20.3 (5.5)	12.3 (10.1)	9.0 (2.3)
2	14 perivenous 2 fused perivenous	7/16	NA	21.7 (19.7)	15.9 (11.8)	4.1 (4.3)	9.5 (5.9)	25.5 (10.9)
3	2 perivenous 1 fused perivenous	1/3	NA	18.6 (14.2)	11.1 (6.5)	6.3 (3.1)	0.8 (1.0)	25.8 (3.2)
4	14 perivenous	14/14	NA	15.7 (24.0)	8.2 (10.2)	6.5 (8.5)	7.6 (14.9)	15.8 (5.2)
5	56 perivenous 2 fused perivenous	4/58	NA	13.3 (8.4)	5.4 (3.3)	4.4 (3.9)	0.1 (0.4)	23.1 (6.7)
6	8 perivenous 1 subpial	5/8	1/1	8.9 (3.5)	5.1 (2.0)	3.9 (0.6)	1.2 (1.8)	10.7 (6.4)
7	24 perivenous 1 fused perivenous 2 large confluent	10/27	NA	10.9 (6.5)	5.8 (4.1)	3.1 (1.3)	2.2 (1.8)	12.0 (6.3)
8	9 perivenous 1 fused perivenous	10/10	NA	32.7 (29.6)	22.8 (23.2)	15.5 (9.3)	7.8 (11.7)	7.5 (1.6)
9	Totally demyelinating lesion	NA	NA	8.9 (6.5)	4.2 (2.1)	3.6 (1.2)	0.5 (0.3)	15.1 (5.9)
10	20 perivenous 4 fused perivenous	7/25	NA	31.1 (13.8)	13.1 (5.3)	14.7 (6.1)	4.8 (1.8)	24.1 (15.6)
11	3 perivenous 1 subpial	2/3	1/1	25.2 (10.9)	17.1 (10.1)	7.7 (4.1)	8.1 (6.3)	9.0 (4.6)

Values are presented as mean cell counts of each cell population/1000 μm^2 (SD).
NA = not applicable.

share an ADEM-like pathology associated with MOG antibody, regardless of the clinical diagnoses.

Demyelination patterns in other inflammatory demyelinating diseases

We compared the demyelinating patterns of MOG antibody-associated disease with other those of inflammatory demyelinating diseases (prototypic multiple sclerosis, TDD with confluent demyelination, AQP4 antibody-positive NMOSD, and the acute phase of ADEM).

In our cases of TDD, CD4 and CD8 T cells infiltrating in the tissues were similar to chronic active cases of multiple sclerosis, and in fact one TDD patient experienced a relapse. All patients with TDD were biopsied during the acute phase and showed the confluent pattern of demyelination without MOG-dominant myelin loss. The activity of macrophages phagocytosing myelin debris, especially at the edge of demyelination plaques, was more evident in patients with TDD with confluent demyelination than in those with MOG antibody-associated demyelination. All autopsied cases of prototypic multiple sclerosis in this study were in the progressive phase and the brain lesions showed a confluent demyelination pattern.

The pathology of AQP4 antibody-positive NMOSD patients was distinct from that of patients with MOG antibody-associated disease in terms of the severe astrocytic damage seen in the former. Additionally, the pathological features of the demyelination pattern in patients with AQP4 antibody-positive NMOSD were demyelination with the preferential loss of MAG and oligodendrocyte loss (Supplementary Fig. 1G–I), which was different from MOG antibody-associated demyelination with relatively preserved oligodendrocytes. In addition, >21% (212/974 vessels) of the active demyelinating lesions in patients with AQP4 antibody-positive NMOSD were accompanied by the perivascular deposition of activated complement components.

All five patients with ADEM with or without an unknown serostatus of MOG antibody showed perivenous demyelination. Interestingly, the demyelination pattern in those patients with ADEM was similar to that of patients with MOG antibody-associated disease, and two of five patients with ADEM showed MOG-dominant myelin loss (Supplementary Fig. 3A–F). However, the MOG antibody serostatus of those two patients was determined in the chronic stable phase of the disease because in those patients, the disease onset occurred long before the establishment of cell-based assays to detect the conformation-sensitive MOG antibody (disease onset in these two patients occurred in 2001 and 2011, respectively, and the MOG antibody was detected in 2018 in both patients and was found to be absent). MOG-dominant demyelination was not observed in a patient in whom MOG antibody seronegativity was confirmed in the serum obtained at the time of disease onset.

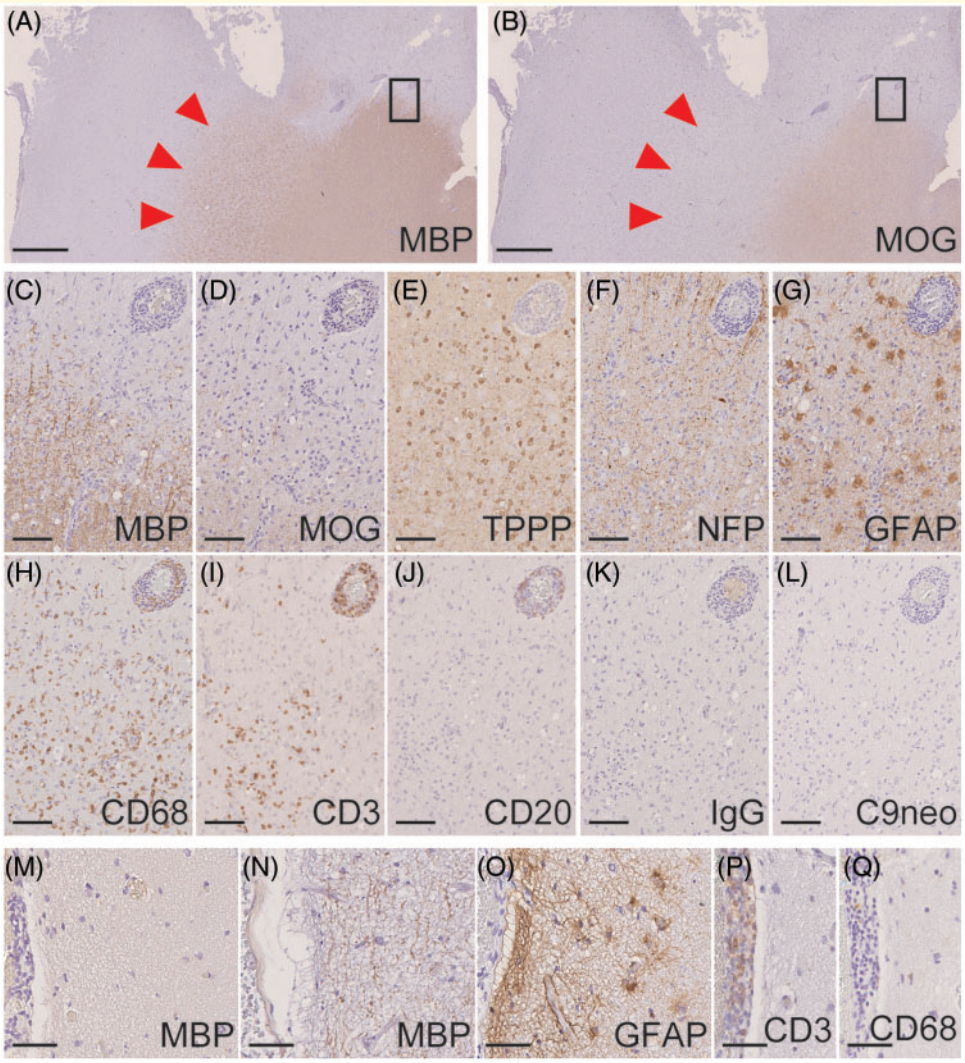

Figure 4 Characteristic features of demyelination at the corticomedullary junction in MOG antibody-associated disease. (**A** and **B**) MOG-dominant subcortical demyelination. The loss of MOG staining (**B**) was more extensive than the loss of MBP staining (**A**). Red arrowheads indicate the border between the loss of MOG and the remaining unaffected white matter in the lower right region (Patient 1). Scale bar = 1000 μm. (**C**–**L**) High magnification images of a selected area indicated by the rectangle in **A** and **B**. (**C** and **D**) The staining of MBP (**C**) was relatively preserved compared with that of MOG (**D**). Scale bar = 100 μm. (**E** and **F**) TPPP+ oligodendrocytes (**E**) and NFP+ axons (**F**) were well preserved even in the demyelinated area. Scale bar = 100 μm. (**G**) Reactive GFAP+ astrocytes were present in the demyelinating area. Scale bar = 100 μm. (**H**) CD68+ macrophages were seen at the border of the demyelinating area. Scale bar = 100 μm. (**I** and **J**) Infiltrated cells were predominantly CD3+ T cells (**I**) rather than CD20+ B cells (**J**). Scale bar = 100 μm. (**K** and **L**) IgG (**K**) and activated complement components (C9neo, **L**) were rarely seen as degraded debris in macrophages in the demyelinating lesions. Scale bar = 100 μm. (**M** and **O**–**Q**) Subpial demyelination. Meninges can be seen on the *left* (Patient 1). (**M**) Myelin sheaths were not stained with MBP in the subpial area. Scale bar = 50 μm. (**N**) The normal staining pattern of MBP in the subpial cortex is shown. Scale bar = 50 μm. (**O**) GFAP+ astrocytes were seen in the subpial cortex. Scale bar = 50 μm. (**P**) CD3+ T cells infiltrated the meninges (scale bar = 50 μm), but relatively rare CD68+ macrophages (**Q**). Scale bar = 50 μm. NFP = neurofilament protein.

The characteristics of the demyelination pattern, complement deposition and inflammatory cell infiltration in each inflammatory demyelinating disease are summarized in Table 3.

Discussion

In this study, we found that the pathology in the majority of patients with MOG antibody-associated disease was characterized by ADEM-like perivenous demyelination in multiple/disseminated lesions with dominant loss of MOG compared with other myelin proteins such as MBP and MAG, but not by multiple sclerosis-like confluent demyelination (Young *et al.*, 2010; Popescu and Lucchinetti, 2012). Those features were consistent regardless of the clinical diagnoses (ADEM, MDEM, cortical encephalitis, leukoencephalopathy, or multifocal lesions without encephalopathy). These results agree well with the fact that the MOG

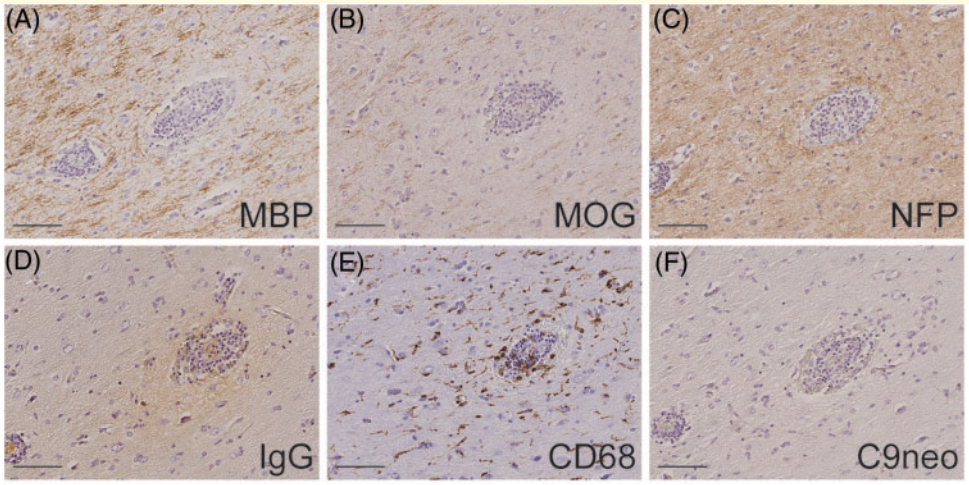

Figure 5 MOG-dominant myelin loss with IgG deposition. (**A**–**C**) Focal perivascular MOG-dominant myelin loss (**B**) compared with MBP (**A**) and preserved NFP (**C**) was seen in the subcortical region accompanied by IgG deposition (**D**) and infiltration by macrophages (**E**). Activated complement components were not seen in this lesion (**F**). [Patient 1, MBP (**A**), MOG (**B**), NFP (**C**), IgG (**D**), CD68 (**E**), C9neo (**F**)]. Scale bar = 100 μm. NFP = neurofilament protein.

antibody is rarely detected in typical multiple sclerosis cases (Di Pauli *et al.*, 2011; Hacohen *et al.*, 2015; Ketelslegers *et al.*, 2015; Kim *et al.*, 2015; Waters *et al.*, 2015). Therefore, we propose that perivenous localization of MOG-dominant demyelination is one of the essential pathological features of MOG antibody-associated disease, which is similar to the vasculocentric loss of AQP4 and GFAP (glial fibrillary acidic protein) in AQP4 antibody-positive NMOSD (Misu *et al.*, 2006, 2007) but is quite different from prototypic multiple sclerosis with chronic expanding demyelinating lesions with activated macrophages at the periphery.

Another important finding in this study is that demyelinating lesions found in patients with MOG antibody-associated diseases exhibit MOG-dominant myelin loss especially in early-stage lesions with the activity of myelin phagocytosing macrophages. In addition, we observed that myelin phagocytosed by some macrophages and debris of myelin components localized at perivascular area near demyelinating lesions were MOG-dominant. On the other hand, in areas lacking MOG staining without marked infiltration of phagocytic macrophages, we cannot exclude the possibility of other pathomechanisms such as internalization or downregulation of MOG molecules. A similar finding is observed in AQP4-IgG-positive NMOSD in which loss of AQP4 (type 4) without astrocyte or tissue damage occurred possibly as a result of antibody-dependent downregulation of AQP4 in the absence of complement activation (Misu *et al.*, 2013). These findings support that MOG antibody-associated disease actually targets MOG to cause autoimmune-mediated demyelination. In addition, relative preservation of oligodendrocytes was confirmed in relatively large demyelinating lesions in MOG antibody-associated disease (Fig. 4E and Supplementary Fig. 1C). As MOG is expressed on the outermost layer of the myelin sheath, MOG antibody-associated demyelination may initially occur on the surface of the myelin sheath. These pathological findings of MOG antibody-associated demyelination are clearly distinct from the demyelination pattern of AQP4 antibody-positive NMOSD, which is characterized by a marked reduction in oligodendrocytes and the loss of MAG (Bruck *et al.*, 2012), which are the characteristics of primary distal oligodendrogliopathy. In contrast to multiple sclerosis, TDD and AQP4 antibody-positive NMOSD, the five patients with ADEM in this study displayed characteristics similar to those of patients with MOG antibody-associated disease, displaying both a perivascular demyelination pattern and MOG-dominant myelin loss. Among them, only one ADEM patient was confirmed to be MOG antibody-negative at the time of disease onset, while the other patients were tested for the MOG antibody long after the brain biopsy had been taken. In some patients who are positive for the MOG antibody, the antibody titres decline over time and may convert to seronegativity in the chronic stage. In addition, the current cell-based assays for MOG antibody detection is highly specific (Waters *et al.*, 2015), but false negative results may occur. Thus, it is possible that our ADEM patients with perivenous demyelination and MOG-dominant myelin loss might have been positive for the MOG antibody if their serostatus had been examined at the time of the onset of the disease.

In the present analysis of cellular immunity, we found CD4+ T cell-dominant inflammatory cell infiltration in the lesions of patients with MOG antibody-associated disease and AQP4 antibody-positive NMOSD; this characteristic is different from the dominance of CD8+ T cell infiltrates observed in multiple sclerosis lesions (Hohlfeld *et al.*, 2016; Machado-Santos *et al.*, 2018). Some of those CD4+ T cells that infiltrated the demyelinating lesions of

Table 3 Comparison of neuropathological findings in MOG antibody-associated diseases and other inflammatory demyelinating diseases in the present study

Disease	Case, *n*	Material	Autoantibody	Demyelination pattern		Stage	Myelin phagocytosis	Oligodendrocyte	Astrocyte	Complement deposition		Infiltrating immune cells			
				PVD	CD					PV	Pa/M	T cells			B cells
												CD3	CD4	CD8	CD20
MOG-antibody- associated disease	11	Biopsy	MOG	++	–~+	Active	+	Preserved	Reactive	±	±	22.9 (19.5)	12.8 (12.0)	8.5 (7.6)	4.7 (8.2)
ADEM (acute phase)	5	Biopsy	–	++	–	Active	+	Preserved	Reactive	–	–	30.4 (27.4)	18.1 (21.7)	10.1 (8.5)	12.4 (12.7)
TDD (acute phase)	4	Biopsy	–	±	++	Active	+++	Partially loss	Reactive	–	–	47.1 (42.1)	23.4 (28.9)	26.4 (26.4)	9.6 (11.9)
Multiple sclerosis (chronic phase)	11	Autopsy	–	–	++	Chronic	+	Loss/regenerate	Reactive	–	–~+	11.2 (28.9)	6.2 (15.6)	8.7 (19.9)	4.0 (23.5)
NMOSD (acute phase)	4	Autopsy	AQP4	+~++	++	Active	++	Loss	Loss	+++	++	23.7 (19.8)	13.5 (14.0)	9.0 (8.8)	4.1 (6.3)
NMOSD (chronic phase)	4	Autopsy	AQP4	–	++	Chronic	±	Loss/regenerate	Loss/ regenerate	±	±	12.3 (14.2)	4.8 (6.3)	5.9 (6.0)	0.8 (1.2)

Demyelination pattern: – = absent; ± = a few; + = present; ++ = many.
Myelin phagocytosis and complement deposition: – = absent; ± = a few; + = mild; ++ = moderate; +++ = severe.
The degree of infiltrating immune cells = mean cell counts of each cell population/1000 μm^2 (SD).
CD = confluent demyelination; Pa/M = parenchyma or macrophage type deposition; PV = perivenous; PVD = perivenous demyelination.

MOG antibody-positive patients might be reactive to MOG epitopes. Moreover, we recently reported that the levels of T helper 17 (Th17)-related cytokines, including IL-6, IL-8 and GM-CSF, were markedly elevated in the CSF during the acute phase of MOG antibody-associated disease and AQP4 antibody-positive NMOSD when compared with the levels in patients with multiple sclerosis (Kaneko *et al.*, 2018). It would be interesting to determine if CD4+ T cells that had infiltrated the perivenous demyelinating lesions in MOG antibody-associated disease are generally positive for Th17. If that is the case, therapies to suppress Th17 may be potentially effective in combating MOG antibody-associated disease, and it would be reasonable to conclude that disease-modifying drugs used to treat multiple sclerosis, such as interferon-beta, are probably ineffective for treating MOG antibody-associated disease, as has been observed in patients with AQP4 antibody-positive NMOSD (Axtell *et al.*, 2011; Jarius *et al.*, 2016*a*, *b*).

Although the deposition of activated complement components, which is an essential feature of multiple sclerosis pathology pattern II (Lucchinetti *et al.*, 2000), was emphasized as a characteristic pathological finding of MOG antibody-associated disease in the previous case reports (Supplementary Tables 2 and 3) (Spadaro *et al.*, 2015; Jarius *et al.*, *2016a*, *b*; Kortvelyessy *et al.*, 2017; Weber *et al.*, 2018), such a humoral immune response was only rarely observed in perivascular areas in this study. This discrepancy may reflect the pathological diversity of MOG antibody-associated disease or may be because these findings are quite short-lived and we excluded them because of the late timing of brain biopsy. However, the finding is in line with reports that the deposition of antibodies and complement components in ADEM patients was limited compared with that observed in patients with multiple sclerosis and NMOSD (Wingerchuk and Lucchinetti, 2007) and that there are some patients with ADEM without the deposition of C9neo (Hoche *et al.*, 2011). In addition, the timing of the brain biopsy might possibly contribute to the different findings. As the majority of our patients were biopsied within 1 month of their first attack, with no prior immunosuppressive treatment, the histopathological findings probably reflect an early stage of the disease. Meanwhile, previous reports included a patient being treated with rituximab (Spadaro *et al.*, 2015) and another without a detailed clinical course described in the article (Jarius *et al.*, *2016a*, *b*). In these patients, confluent demyelinating plaques may be produced by the fusion of perivascular demyelinating lesions over time (Young *et al.*, 2010).

AQP4 antibody is known to be pathogenic by inducing astrocytic damage, but it has not been established how MOG antibody contributes to the pathogenesis of human MOG antibody-associated disease. MOG antibody is mainly IgG1 and can activate complement components (Mader *et al.*, 2011), and MOG antibody has been reported to cause complement-mediated cytotoxicity *in vitro* (Mader *et al.*, 2011), *ex vivo* (Peschl *et al.*, 2017*b*)

and *in vivo* (Spadaro *et al.*, 2018). While a fraction of the demyelinating lesions in our patients with MOG antibody-associated disease were accompanied by complement deposition, such lesions were much rarer than in acute lesions of patients with NMOSD with AQP4-antibody, the IgG subclass of which is also IgG1. The binding affinity of C1q to IgG, which is the first step in complement activation, markedly increases when C1q binds to two or more adjacent IgG molecules (Hughes-Jones, 1977). On the cell surface, M23-AQP4 tetramers assemble to form an orthogonal array of particles on the cell membrane, which can enhance complement-dependent cytotoxicity as AQP4 antibodies tend to cluster on the AQP4 orthogonal array of particles (Phuan *et al.*, 2012). On the other hand, MOG is present on the outermost layer of the myelin sheath, but it comprises <0.05% of the total myelin protein and does not form a special structure such as an orthogonal array of particles (Brunner *et al.*, 1989). Therefore, AQP4 and MOG differ not only in the targets of the autoimmune attacks (astrocytes versus myelin) (Kaneko *et al.*, 2016) but also in the complement-mediated cytotoxicity induced by the autoantibodies. In the present study, we observed that a small number of MOG-dominant demyelinating lesions were accompanied by IgG deposition without activated complement components, which appears to support the experimental finding that MOG antibody purified from the sera of patients can alter the structure of the microtubule cytoskeleton of cultured oligodendrocytes (Dale *et al.*, 2014). In fact, one probable physiological function of MOG is to stabilize cytoskeletal microtubules (Johns and Bernard, 1999). Moreover, MOG antibodies can cause reversible myelin changes independent of complement components *in vivo* (Saadoun *et al.*, 2014). Taken together, MOG antibodies by themselves may cause myelin degeneration in a complement-independent manner under specific conditions.

The present study has some limitations. First, as we pathologically examined only 11 brain biopsies from patients with MOG antibody-associated disease, we might not have captured the full pathological spectrum of the disease, especially with regard to the chronic stage. Consistent histopathological findings seen across the patients with MOG antibody-associated disease strongly suggest that they represent the uniqueness of this clinical entity, but larger-scale pathological studies of autopsy materials may provide further insights to generate a better understanding of MOG antibody-associated disease and better therapeutic management of the patients. Second, only brain lesions were analysed in our study, but it is important to study lesions in the optic nerve and spinal cord to clarify if their pathological characteristics are similar to those of the brain lesions. Third, in this kind of immunohistochemical study, tissue and cellular staining can be influenced by several factors such as tissue fixation, antigen retrieval and the antibodies used in the methods. Therefore, different immunohistochemical methods may generate different immunostaining densities and patterns.

Conclusion

Our study suggests that ADEM-like perivenous disseminated inflammatory demyelination with MOG-dominant myelin loss with preserved oligodendrocytes, CD4-dominant T cell infiltration, and perivascular MOG-laden macrophages are characteristic findings in the acute phase of MOG antibody-associated disease. These pathological features were clearly different from those of multiple sclerosis and AQP4 antibody-positive NMOSD, suggesting that MOG antibody-associated disease is an independent autoimmune demyelinating disease targeting MOG.

Acknowledgements

We thank the clinicians and pathologists who sent us the brain tissue specimens and especially Drs Hikaru Kitahara and Yo Okizuka of Takatsuki Hospital, Dr Takayuki Kosaka of National Hospital organization Kumamoto Medical Center, Drs Tomoyo Hashimoto and Kazumasa Okada of the University of Occupational and Environmental Health, and Professor Jin Nakahara of Keio University for referring the patients to us. The authors also thank Ms Koran Ito for providing technical assistance.

Funding

This study was supported in part by KAKENHI (#17K16108, #17H04192, #15K09332) from the Ministry of Education, Culture, Sports, Science and Technology (MEXT) of Japan and the Grants-in-Aid for Scientific Research from the Ministry of Health, Labour and Welfare of Japan.

Competing interests

The authors report no competing interests.

Supplementary material

Supplementary material is available at *Brain* online.

Appendix 1

Japan MOG-antibody Disease Consortium collaborators

Yoshihisa Otsuka, Keiichi Nishimaki, Sho Ishigaki, Kazunari Yoshida, Yasuyuki Iguchi, Takahiro Fukuda, Seitaro Nohara, Akira Tamaoka, Juichi Fujimori.

References

Axtell RC, Raman C, Steinman L. Interferon-beta exacerbates Th17-mediated inflammatory disease. Trends Immunol 2011; 32: 272–7.

Bruck W, Popescu B, Lucchinetti CF, Markovic-Plese S, Gold R, Thal DR, et al. Neuromyelitis optica lesions may inform multiple sclerosis heterogeneity debate. Ann Neurol 2012; 72: 385–94.

Brunner C, Lassmann H, Waehneldt TV, Matthieu JM, Linington C. Differential ultrastructural localization of myelin basic protein, myelin/oligodendroglial glycoprotein, and 2',3'-cyclic nucleotide 3'-phosphodiesterase in the CNS of adult rats. J Neurochem 1989; 52: 296–304.

Dale RC, Tantsis EM, Merheb V, Kumaran RY, Sinmaz N, Pathmanandavel K, et al. Antibodies to MOG have a demyelination phenotype and affect oligodendrocyte cytoskeleton. Neurol Neuroimmunol Neuroinflamm 2014; 1: e12.

Di Pauli F, Mader S, Rostasy K, Schanda K, Bajer-Kornek B, Ehling R, et al. Temporal dynamics of anti-MOG antibodies in CNS demyelinating diseases. Clin Immunol 2011; 138: 247–54.

Fujimori J, Takai Y, Nakashima I, Sato DK, Takahashi T, Kaneko K, et al. Bilateral frontal cortex encephalitis and paraparesis in a patient with anti-MOG antibodies. J Neurol Neurosurg Psychiatry 2017; 88: 534–6.

Hacohen Y, Absoud M, Deiva K, Hemingway C, Nytrova P, Woodhall M, et al. Myelin oligodendrocyte glycoprotein antibodies are associated with a non-MS course in children. Neurol Neuroimmunol Neuroinflamm 2015; 2: e81.

Hoche F, Pfeifenbring S, Vlaho S, Qirshi M, Theis M, Schneider W, et al. Rare brain biopsy findings in a first ADEM-like event of pediatric MS: histopathologic, neuroradiologic and clinical features. J Neural Transm 2011; 118: 1311–7.

Hohlfeld R, Dornmair K, Meinl E, Wekerle H. The search for the target antigens of multiple sclerosis, part 2: CD8+ T cells, B cells, and antibodies in the focus of reverse-translational research. Lancet Neurol 2016; 15: 317–31.

Hughes-Jones NC. Functional affinity constants of the reaction between 125I-labelled C1q and C1q binders and their use in the measurement of plasma C1q concentrations. Immunology 1977; 32: 191–8.

Ikeda T, Yamada K, Ogawa R, Takai Y, Kaneko K, Misu T, et al. The pathological features of MOG antibody-positive cerebral cortical encephalitis as a new spectrum associated with MOG antibodies: a case report. J Neurol Sci 2018; 392: 113–5.

Jarius S, Metz I, Konig FB, Ruprecht K, Reindl M, Paul F, et al. Screening for MOG-IgG and 27 other anti-glial and anti-neuronal autoantibodies in 'pattern II multiple sclerosis' and brain biopsy findings in a MOG-IgG-positive case. Mult Scler 2016a; 22: 1541–9.

Jarius S, Ruprecht K, Kleiter I, Borisow N, Asgari N, Pitarokoili K, et al. MOG-IgG in NMO and related disorders: a multicenter study of 50 patients. Part 2: epidemiology, clinical presentation, radiological and laboratory features, treatment responses, and long-term outcome. J Neuroinflamm 2016b; 13: 280.

Johns TG, Bernard CC. The structure and function of myelin oligodendrocyte glycoprotein. J Neurochem 1999; 72: 1–9.

Kaneko K, Sato DK, Nakashima I, Nishiyama S, Tanaka S, Marignier R, et al. Myelin injury without astrocytopathy in neuroinflammatory disorders with MOG antibodies. J Neurol Neurosurg Psychiatry 2016; 87: 1257–9.

Kaneko K, Sato DK, Nakashima I, Ogawa R, Akaishi T, Takai Y, et al. CSF cytokine profile in MOG-IgG+ neurological disease is similar to AQP4-IgG+ NMOSD but distinct from MS: a cross-sectional study and potential therapeutic implications. J Neurol Neurosurg Psychiatry 2018; 89: 927–36.

Ketelslegers IA, Van Pelt DE, Bryde S, Neuteboom RF, Catsman-Berrevoets CE, Hamann D, et al. Anti-MOG antibodies plead against MS diagnosis in an Acquired Demyelinating Syndromes cohort. Mult Scler 2015; 21: 1513–20.

Kim SM, Woodhall MR, Kim JS, Kim SJ, Park KS, Vincent A, et al. Antibodies to MOG in adults with inflammatory demyelinating disease of the CNS. Neurol Neuroimmunol Neuroinflamm 2015; 2: e163.

Kitley J, Woodhall M, Waters P, Leite MI, Devenney E, Craig J, et al. Myelin-oligodendrocyte glycoprotein antibodies in adults with a neuromyelitis optica phenotype. Neurology 2012; 79: 1273–7.

Koelman DL, Mateen FJ. Acute disseminated encephalomyelitis: current controversies in diagnosis and outcome. J Neurol 2015; 262: 2013–24.

Komatsu T, Matsushima S, Kaneko K, Fukuda T. Perivascular enhancement in anti-MOG antibody demyelinating disease of the CNS. J Neurol Neurosurg Psychiatry 2019; 90: 111–2.

Kortvelyessy P, Breu M, Pawlitzki M, Metz I, Heinze HJ, Matzke M, et al. ADEM-like presentation, anti-MOG antibodies, and MS pathology: TWO case reports. Neurol Neuroimmunol Neuroinflamm 2017; 4: e335.

Lassmann H, Brunner C, Bradl M, Linington C. Experimental allergic encephalomyelitis: the balance between encephalitogenic T lymphocytes and demyelinating antibodies determines size and structure of demyelinated lesions. Acta Neuropathol 1988; 75: 566–76.

Linington C, Bradl M, Lassmann H, Brunner C, Vass K. Augmentation of demyelination in rat acute allergic encephalomyelitis by circulating mouse monoclonal antibodies directed against a myelin/oligodendrocyte glycoprotein. Am J Pathol 1988; 130: 443–54.

Lucchinetti C, Bruck W, Parisi J, Scheithauer B, Rodriguez M, Lassmann H. Heterogeneity of multiple sclerosis lesions: implications for the pathogenesis of demyelination. Ann Neurol 2000; 47: 707–17.

Machado-Santos J, Saji E, Troscher AR, Paunovic M, Liblau R, Gabriely G, et al. The compartmentalized inflammatory response in the multiple sclerosis brain is composed of tissue-resident CD8+ T lymphocytes and B cells. Brain 2018; 141: 2066–82.

Mader S, Gredler V, Schanda K, Rostasy K, Dujmovic I, Pfaller K, et al. Complement activating antibodies to myelin oligodendrocyte glycoprotein in neuromyelitis optica and related disorders. J Neuroinflamm 2011; 8: 184.

Misu T, Fujihara K, Kakita A, Konno H, Nakamura M, Watanabe S, et al. Loss of aquaporin 4 in lesions of neuromyelitis optica: distinction from multiple sclerosis. Brain 2007; 130: 1224–34.

Misu T, Fujihara K, Nakamura M, Murakami K, Endo M, Konno H, et al. Loss of aquaporin-4 in active perivascular lesions in neuromyelitis optica: a case report. Tohoku J Exp Med 2006; 209: 269–75.

Misu T, Höftberger R, Fujihara K, Wimmer I, Takai Y, Nishiyama S, et al. Presence of six different lesion types suggests diverse mechanisms of tissue injury in neuromyelitis optica. Acta Neuropathol 2013; 125: 815–27.

Ogawa R, Nakashima I, Takahashi T, Kaneko K, Akaishi T, Takai Y, et al. MOG antibody-positive, benign, unilateral, cerebral cortical encephalitis with epilepsy. Neurol Neuroimmunol Neuroinflamm 2017; 4: e322.

Peschl P, Bradl M, Hoftberger R, Berger T, Reindl M. Myelin oligodendrocyte glycoprotein: deciphering a target in inflammatory demyelinating diseases. Front Immunol 2017a; 8: 529.

Peschl P, Schanda K, Zeka B, Given K, Bohm D, Ruprecht K, et al. Human antibodies against the myelin oligodendrocyte glycoprotein can cause complement-dependent demyelination. J Neuroinflammation 2017b; 14: 208.

Phuan PW, Ratelade J, Rossi A, Tradtrantip L, Verkman AS. Complement-dependent cytotoxicity in neuromyelitis optica requires aquaporin-4 protein assembly in orthogonal arrays. J Biol Chem 2012; 287: 13829–39.

Popescu BF, Lucchinetti CF. Pathology of demyelinating diseases. Annu Rev Pathol 2012; 7: 185–217.

Ramanathan S, Dale RC, Brilot F. Anti-MOG antibody: the history, clinical phenotype, and pathogenicity of a serum biomarker for demyelination. Autoimmun Rev 2016; 15: 307–24.

Reindl M, Di Pauli F, Rostsy K, Berger T. The spectrum of MOG autoantibody-associated demyelinating diseases. Nat Rev Neurol 2013; 9: 455–61.

Saadoun S, Waters P, Owens GP, Bennett JL, Vincent A, Papadopoulos MC. Neuromyelitis optica MOG-IgG causes reversible lesions in mouse brain. Acta Neuropathol Commun 2014; 2: 35.

Sato DK, Callegaro D, Lana-Peixoto MA, Waters PJ, de Haidar Jorge FM, Takahashi T, et al. Distinction between MOG antibody-positive and AQP4 antibody-positive NMO spectrum disorders. Neurology 2014; 82: 474–81.

Spadaro M, Gerdes LA, Mayer MC, Ertl-Wagner B, Laurent S, Krumbholz M, et al. Histopathology and clinical course of MOG-antibody-associated encephalomyelitis. Ann Clin Transl Neurol 2015; 2: 295–301.

Spadaro M, Winklmeier S, Beltran E, Macrini C, Hoftberger R, Schuh E, et al. Pathogenicity of human antibodies against myelin oligodendrocyte glycoprotein. Ann Neurol 2018; 84: 315–28.

Takahashi T, Fujihara K, Nakashima I, Misu T, Miyazawa I, Nakamura M, et al. Establishment of a new sensitive assay for anti-human aquaporin-4 antibody in neuromyelitis optica. Tohoku J Exp Med 2006; 210: 307–13.

Waters P, Woodhall M, O'Connor KC, Reindl M, Lang B, Sato DK, et al. MOG cell-based assay detects non-MS patients with inflammatory neurologic disease. Neurol Neuroimmunol Neuroinflamm 2015; 2: e89.

Weber MS, Derfuss T, Metz I, Bruck W. Defining distinct features of anti-MOG antibody associated central nervous system demyelination. Ther Adv Neurol Disord 2018; 11: 1756286418762083.

Wingerchuk DM, Lucchinetti CF. Comparative immunopathogenesis of acute disseminated encephalomyelitis, neuromyelitis optica, and multiple sclerosis. Curr Opin Neurol 2007; 20: 343–50.

Young NP, Weinshenker BG, Parisi JE, Scheithauer B, Giannini C, Roemer SF, et al. Perivenous demyelination: association with clinically defined acute disseminated encephalomyelitis and comparison with pathologically confirmed multiple sclerosis. Brain 2010; 133: 333–48.